Int. J. Electrochem. Sci., 9 **(2014)** 6896 - 6909

International Journal of
ELECTROCHEMICAL
SCIENCE
www.electrochemsci.org

Detection of antiemetic drug based on Semiconductor Metal Oxide Nanostructures onto Micro-chips by Electrochemical Approach

Mohammed M. Rahman[1,2,*], *Abdullah M. Asiri*[1,2], *Sher Bahadar Khan*[1,2]

[1] Center of Excellence for Advanced Materials Research (CEAMR), King Abdulaziz University, Jeddah 21589, P.O. Box 80203, Saudi Arabia;
[2] Chemistry Department, Faculty of Science, King Abdulaziz University, P.O. Box 80203, Jeddah 21589, Saudi Arabia
[*]E-mail: mmrahman@kau.edu.sa; mmrahmanh@gmail.com

Received: 4 August 2014 / *Accepted:* 11 September 2014 / *Published:* 29 September 2014

We have prepared calcined Ag_2O nanoparticles (NPs) by a wet-chemical method using reducing agents in alkaline medium. The NPs were characterized by UV/vis., FT-IR, X-ray photoelectron spectroscopy (XPS), X-ray powder diffraction (XRD), Energy-dispersive X-ray spectroscopy, and Field-Emission Scanning Electron Microscopy (FESEM) etc. NPs were embedded onto μ-chips to fabricate a sensor with a fast response towards aprepitant (APPT) in phosphate buffer phase. The fabricated APPT sensor on NPs/μ-chips also exhibits higher sensitivity, low-sample volume, reliable, reproducibility, easy integration, long-term stability, and enhanced electrochemical responses. The calibration plot is linear (r^2 = 0.9852) over the large APPT concentration ranges (2.2 nM to 4.1 μM). The sensitivity and detection limit is calculated as ~2.732 $\mu Acm^{-2}\mu M^{-1}$ and ~0.29 nM (SNR of 3) respectively. Here, it is also discussed the possible potential uses of the NPs in terms of APPT sensing, which could also be employed for the determination of biochemicals in quality control of formulation.

Keywords: Aprepitant; Ag_2O Nanoparticles; μ-Chips; Optical properties; Sensitivity

1. INTRODUCTION

Aprepitant (APPT, 5-[[(2R,3S)-2-[(1R)-1-[3,5-bis(trifluoromethyl)phenyl]ethoxy]-3-(4-fluorophenyl)-4-morpholinyl]methyl]-1,2dihydro-3H-1,2,4-triazol-3-one]) is an antiemetic chemical-compound that belongs to a class of drugs called substance-P-antagonists, which mediates its effect by blocking the neurokinin 1 (NK_1) receptor. APPT is a selective high affinity antagonist of human-substance that has little or no affinity for serotonin (5-HT3), dopamine, and corticosteroid receptors. A large number of drugs are available for prevention of postoperative nausea and vomiting [1,2], which

5-HT3 receptor antagonists have occupied an important position because of their better efficiency and side-effect profile with a disadvantage that prevents only acute emesis. A newer class of drugs namely neurokinin receptor antagonists provide a supplementary benefit of inhibiting both-acute and delayed-emesis. The brain-penetrant, selective NK1 receptor antagonist APPT was extended for utilize in combination with a 5HT3 receptor antagonist and a corticosteroid for the prevention of chemo-therapy induced nausea and vomiting [3,4**]**. The recommended doses of APPT in this regimen are a single oral capsule on the day of chemo-therapy. The antiemetic efficacy of oral APPT in the setting of CINV is well documented [5,6]. Although the oral capsule is appropriate for many patients, the accessibility of an intravenous (IV) alternative would offer greater treatment flexibility and convenience when the oral way of administration is not feasible, such as in patients with impaired consciousness or those with disease related nausea who cannot tolerate drugs by mouth. Anticancer dealing focused on cisplatin chemo-therapy is related with unfriendly and distressing side effects, which decrease the expectancy of life and may cause patients to delay or refuse possibly curative therapy [7,8]. Efforts to inhibit chemo-therapy induced emesis have been engaged at hindering neuro-transmitter receptors (dopamine, serotonin, and substance-P) in the brain stem vomiting center. APPT (neurokinin-1) receptor antagonist that directly mediates the biological actions of substance-P, is currently in clinical progress for chemo-therapy induced emesis [9]. In a double-blind, placebo-controlled clinical trial, APPT was shown to prevent delayed emesis after treatment with cisplatin [10]. Though newer routes of drug detection are constantly being improved, solid-dosage forms continue to be the most popular delivery vehicle for pharmaceutically active therapeutic agents [11]. Chemical and physical properties of solid active ingredients can play a very important role in their process-ability and bioavailability. Different polymorphs of the APPT drug are different not only in their crystal shape and structure but also in their solubility, melting point, thermodynamic stability, density, vapor pressure, and electrical properties. HPLC chromatographic reactor methodology for examining the hydrolytic stability of a pharmaceutical compound [12], estimation of APPT in rhesus macaque plasma [13], characterization and quantification of APPT drug substance polymorphs by attenuated total reflectance FT-IR [14], stability of an extemporaneous oral liquid APPT formulation [15], estimation of APPT capsules by RP-HPLC [16] were reported. The objective of this work was to develop a new, simple, economic, rapid, precise, and accurate stability-indicating HPLC method for quantitative analysis of APPT, and to validate the method in accordance with ICH guidelines [17-21] with rimonabant hydrochloride as an internal standard showed advantages of shorter retention time, runtime, and economic steps [22-29].

Silver oxide nanostructures have attracted significant consideration because of their potential application in fabricating nano-scale electronics, optical to biological micro-devices, electron field emission sources for emission displays, and the surface enhanced Raman property with controlled shape and morphology [30-33]. Recently it has fabricated in the pores of anodic aluminum oxide film and poly-carbonate track etched membrane by electrochemical deposition [34]. Silver oxide forms a wide group of compounds that fascinated significant interest, generally due to the wide-spread existence of Ag_2O and Ag_4O_4. For Ag_4O_4, it is used higher reduction potential as cathodic material in Zn–silver oxide in particular applications [36-37]. Conversely, the bacterio-static properties of Ag_2O powder have been previously used for application in the treatment and cure of dermatological skin conditions [38]. Specific surface area of Ag_2O nanostructure plays an important role for powerful antimicrobial applications due to very high charge/discharge ratio [39,40]. Increase of the specific active-surface, it can be obtained by controlling the silver oxide nanostructure (i.e. morphology and

porosity) in the micro-scale. Several research groups already reported that Ag_2O nanostructures could be fabricated with several ways, such as solid–liquid phase, arc-discharge, ultra-violet irradiation, and photo-reduction [41-47]. B.H. Hong et al. published that silver wires with narrow width grew up to micro-scale length inside the pores of calyx-4-hydroquinone tubes by electro-photochemical reaction in a liquid phase [48]. Suwen Liu et al. evaluated a reduction method to make long, straight Ag nanowires by nano-crystalline AgBr and a developer containing silver nitrate component as pre-cursors [49]. Murphy et al. have recently investigated the preparation of Ag-nano-wires by controlling the amount of sodium hydroxide added to the reaction medium, without the use of any surfactants/polymers [50,51]. Beside this, other techniques were also used to synthesize Ag-nanowires [52,53]. In common, various morphologies and thick-nesses are needed when oxides films are employed for different applications. A highly porous thin-film with large-surface area can improve the catalytic efficiency. Several techniques including chemical-vapor deposition, ion-sputtering, and sol–gel have been used for the preparation of oxides thin-films. However, there are several methods having the advantages of by a single processing unit to control the morphology and thickness of metal oxides thin films. Therefore, the development of a reliable method that can make oxides films with controllable morphology and thickness for various reasons is important. In particular, metal oxides based thin films have promising applications in optics as protective barriers. This coating can be used to offer specific optical properties in glasses (anti-reflection, selective reflection, photo-chromism, etc.), to prevent chemical corrosion and gas oxidation in metals, and even in functional applications such as oxygen sensors or buffer layers in micro-electronic devices [54-56]

Nanostructure material is extensively employed for the detection of drug biomolecules in chemical control process owing to their several benefits over conventional chemical analysis techniques in terms of higher response, large-surface area, portability, and monitoring of healthcare and biomedical fields. In conventional electrochemical method with uncoated nanomaterials electrodes for APPT detection, it exhibits the slower response, surface fouling, noise, un-stable signals, and lower dynamic range as well as lower sensitivity. Hence, the modification of the sensor surface with un-doped nanomaterials is very important to attain higher sensitive, repeatable, and stable responses. Therefore, a simple and reliable I-V electrochemical approach is urgently required for relatively easy, convenient, and inexpensive instrumentation which exhibits higher sensitivity and lower detection limits compared to conventional methods. Here, we introduced a very simple, reliable, large-scale, highly sensitive technique for electrochemical detection of APPT drug using silver oxide un-doped nanomaterials at room conditions. The present approach depicts a simple, reliable, highly sensitive, low-sample volume, ease to handle, and precise electrochemical I-V techniques over the existing electrochemical methods, which are free from experimental steps.

2. EXPERIMENTAL SECTIONS

2.1. Materials and Methods

Stock solutions of Aprepitant (APPT, molecular weight, 534.43) were prepared by dissolving 0.022 mg in 10.0 ml of 0.1M phosphate buffer solution (PBS). Volume was made up to mark in a 10.0 ml calibrated volumetric flask with PBS to obtain the stock solution of 0.041 mM of APPT drug.

Amount of 0.1M PBS was kept constant in the beaker as 10.0 mL throughout the chemical investigation. APPT analyte solution is prepared with various concentrations in the range of 2.2. nM to 0.04 mM. The drug sensitivity is calculated from the slope of current vs. concentration (I vs. C) from the calibration plot divided by the value of active surface area of fabricated micro-chip electrodes. Electrometer is used as a voltage sources for I-V technique in two electrode systems. 0.1M phosphate buffer solution (PBS) at pH 7.0 is prepared by mixing of uni-molar concentration of 0.2M Na_2HPO_4 and 0.2M NaH_2PO_4 solution in 100.0 mL de-ionize water at room conditions. Butyl carbitol acetate, silver chloride, ethyl acetate, ammonia solution (25%), and all other chemicals were in analytical grade and purchased from Sigma-Aldrich Company. The λ_{max} (~261.0 nm) of as-grown Ag_2O NPs was executed using UV/visible spectroscopy Lamda-950, Perkin Elmer, Germany. FT-IR spectra of Ag_2O NPs were done on a spectrum-100 FT-IR spectrophotometer in the mid-IR range purchased from Bruker (ALPHA, USA). The XPS measurement of Ag_2O NPs was obtained on a Thermo Scientific K-Alpha KA1066 spectrometer (Germany). A monochromatic AlKα x-ray radiation source was used as excitation sources, where beam-spot size was kept in 300.0 μm. The spectra was recorded in the fixed analyzer transmission mode, where pass energy was kept at ~200 eV. The scanning of the spectra was performed at pressures less 10^{-8} Torr. Morphology, size, and structure of as-grown Ag_2O NPs were recorded on FE-SEM instrument from JEOL (JSM-7600F, Japan). The powder X-ray diffraction (XRD) patterns of Ag_2O NPs were recorded by X-ray diffractometer from PANalytical diffractometer equipped with Cu-$K_{\alpha 1}$ radiation (λ =1.5406 nm) using a generator voltage of 45.0 kV and a generator current of 40.0 mA were applied for the determination. Raman spectrometer was used to measure the Raman shift of as-grown Ag_2O NPs using radiation source (Ar^+ laser line, λ; 513.4 nm), which was purchased from Perkin Elmer (Raman station 400, Perkin Elmer, Germany). I-V technique is executed for the investigation of APPT drugs by using Electrometer (Kethley, 6517A, Electrometer, USA) at room conditions.

2.2. Preparation and growth mechanism of low-dimensional Ag_2O NPs

Liquid-phase precipitation method was used to prepare as-grown nanostructures of Ag_2O by wet-chemical technique from silver chloride with urea as the precipitating agent. Initially, silver chloride (~50.0 ml) was slowly dissolved into the deionized water to make 0.5 M concentration at room temperature. Then the solution was stirred vigorously for 15 minutes. The solution pH was slowly adjusted by drop wise adding of ammonia solution at approximately 9.5. Then the reactant mixture was put in conical flux for 3.0 hours on hot-plate (active temperature, ~92.0^{o}C). Then the final solution was washed with ethanol, acetone, water consequently and kept for drying at room temperature for several hours. The as-synthesized products were characterized in terms of their structural, optical, and electrical properties. The as-grown Ag_2O nanoparticles were applied for the fabrication of APPT drug sensors using micro-chips.

The growth of the silver oxide nanoparticles can be well explained by the thermal reaction concerned and crystal growth behaviors of silver oxide. For the synthesis of silver oxide nanostructures, silver chloride and ammonium hydroxide (as reducing agents) were mixed under

continuous stirring. The reducing agent is controlled the size during growth of silver oxide NPs, which has more important role in thermal reaction systems. During the reaction technique, the NH_4OH performs the major rules, like control the pH value of the solution as well as resource to supply hydroxyl ions into the reaction batch. The $AgCl_2$ reacts with NH_4OH and forms AgOH, which upon heating; further produce into Ag^+ and OH^- ions, which consequently assist in the development of silver oxides according to the following chemical reactions **(i) - (iii).**

$$NH_4OH_{(aq)} \rightarrow NH_4^+{}_{(aq)} + OH^-_{(aq)} \quad \text{(i)}$$

$$AgCl_{2(s)} \rightarrow Ag^+_{(aq)} + 2Cl^-_{(aq)} \quad \text{(ii)}$$

$$Ag^+_{(aq)} + OH^-_{(aq)} \rightarrow AgOH_{(aq)} \quad \text{(iii)}$$

The AgOH finally, however dissociates to form the Ag_2O nuclei at high temperature according to the reactions (iv) - (vi).

$$2Ag^+_{(aq)} + 2OH^-_{(aq)} \rightarrow 2Ag(OH)_{(aq)} \rightarrow Ag_2O_{(s)} + H_2O \quad \text{(iv)}$$

$$AgCl_{2(s)} + NH_4OH_{(aq)} \rightarrow Ag(OH)_{(aq)} + NH_4^+ + 2Cl^-_{(aq)} \quad \text{(v)}$$

$$2Ag(OH)_{(aq)} \rightarrow Ag_2O_{(s)} + H_2O_{(aq)} \quad \text{(vi)}$$

The initially formed Ag_2O nuclei perform as building blocks for the growth of final products. With reaction time under the appropriate thermal conditions, the Ag_2O nuclei concentration enlarges which lead the construction of desired nanostructure products. As the Ag_2O nanostructures are prepared by thermal method, which is supposed that the fundamental unit for the configuration is Ag_2O nanoparticles [57]

2.3. Fabrication and detection of APPT using Ag_2O NPs/μ-chip assembly

Preparation of μ-chip by usual photolithographic method has been investigated in details in the previous report [58-60]. Here, μ-chip is fabricated with Ag_2O NPs using butyl carbitol acetate (BCA) and ethyl acetate (EA) as a conducting binding agent. Then NPs/μ-chip assembly is kept in the oven at 65.0 ^oC for three hours until the film is completely dry, smooth, and uniform. NPs/μ-chip as a working and Pt line (on μ-chip) are worked a counter electrode respectively. As received APPT is diluted to make various concentrations (0.123 μM to 12.3 mM) in DI water and used as a target drug analyte. 70.0 μL of target APPT solution is dropped onto the NPs/μ-chip during sample measurements. The ratio of voltage versus current (slope of calibration curve) is used to measure of APPT drug sensitivity. Detection limit is calculated from the ratio of 3N/S (ratio of noise×3 vs. sensitivity) in the linear dynamic range of calibration plot. In I-V technique, it is used as a voltage sources in Kethley electrometer in simple two-electrode assembly.

3. RESULTS AND DISCUSSION

3.1. Optical characterization of Ag_2O NPs

For UV/visible spectroscopy, the absorption spectrum of Ag_2O NP solution is measured as a function of wavelength, which is presented in Figure 1a. It shows a broad absorption band around

261.0 nm in the visible range between 200.0 to 800.0 nm wavelengths indicated the formation of silver oxide nanostructure materials [61]. The band-gap energy is calculated on the basis of the maximum absorption band of Ag_2O NPs and obtained to be 4.75096 eV, according to following equation (vii) [It is derived from the well-known Plank relation (E=hυ)].

$$E_{bg} = \frac{1240}{\lambda} \text{ (eV)} \quad \text{(vii)}$$

Where E_{bg} is the band gap energy and λ_{max} is the wavelength (261.0 nm) of the Ag_2O NPs.

FT-IR spectrum of Ag_2O NPs with KBr compound is presented in the Figure 1b. It represents band at 682 cm^{-1} at lower frequency ranges. The observed vibration band may be indicated as 682.0 cm^{-1} (Ag-O-Ag stretching vibration). The observed vibrational bands at low frequency regions suggest the formation of Ag_2O NPs by thermo-chemical methods [62].

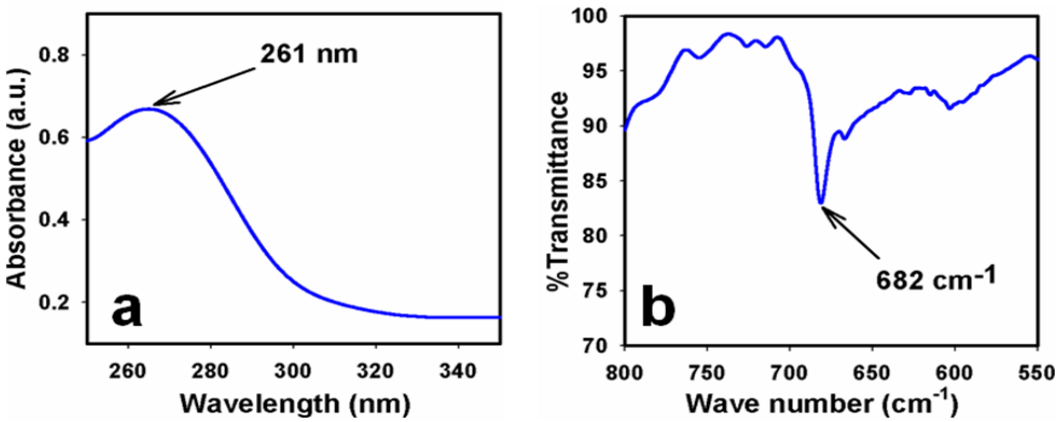

Figure 1. (a) UV/visible and (b) FT-IR spectroscopy of undoped Ag_2O NPs at room conditions**.**

3.2. Morphological, Structural, and Elemental properties of Ag_2O NPs

High-resolution FESEM images of as-grown Ag_2O NPs are revealed in Fig. 2. It shows the FESEM images of the spherical shape and sizes of as-prepared Ag_2O NPs. The diameter of Ag_2O NPs is calculated in the range of 31.82 ~ 50.23 nm. Figure 2(a-b) shows the low to high magnified images of nanoparticles growth by thermo-chemical method, where the average diameters close 38.38 ± 5.0 nm. It is clearly revealed from the FE-SEM images that the prepared products are particle shape in aggregated form, which are grown in a very high-density and possessing almost uniform shape showed in Figure 2(a-b).

The EDS (electron dispersive x-ray spectroscopy) analysis of these nanoparticles indicates the presence of silver and oxygen composition in the pure as-grown silver oxide NPs (Ag_2O). It is clearly displayed that the as-grown prepared materials contained only silver and oxygen elements, which is presented in Figure 2c. No other peak related with any impurity has been detected in the FESEM-EDS,

which confirms that the as-grown nanostructures are composed only with silver (68.89%) and oxygen (31.11%).

X-ray diffraction can be used to determine which Ag_2O NPs are present in materials by calculating or comparing with the standard value of lattice parameters, crystal structures, and crystallinity of JCPDS. The XRD data is presented in the Fig. 2d. It is clearly revealed that all of the peaks match well with the Bragg reflections of the standard face-centered cube structure (Space group: Im-3m, a=2.8839, b=2.8839, c=2.8839), and the three sharp peaks at 38.2 ^{o}, 46.1 ^{o}, and 64.3 ^{o} can be assigned to their characteristic (111), (200), and (220) indices respectively. The three diffraction peaks can be readily indexed to the (111), (200), and (220) planes of fcc silver. It showed that the ratio between the intensities of the (111) and (200) diffraction peaks is relatively higher than the conventional value, indicating that the (111) planes of Ag_2O tend to be preferentially oriented in the experiment system [63]. All the reflected peaks in this pattern were found to match with the Ag_2O phase having face centered cube (JCPDS: 042-0783).

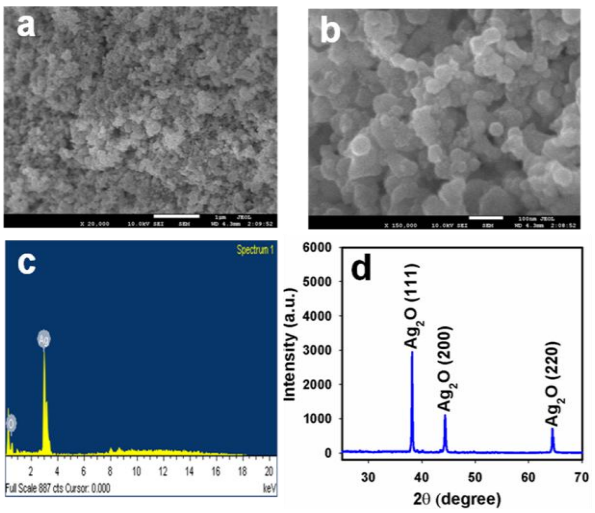

Figure 2. (a-b) FE-SEM images, (c) EDS, and (d) Powder XRD, of calcined Ag_2O NPs at room conditions.

X-ray photoelectron spectroscopy (XPS) is a quantitative spectroscopic technique that determines the chemical-states of the elements that present within undoped silver oxide nanoparticles. XPS spectra are acquired by irradiating on an Ag_2O NPs with a beam of X-rays, while simultaneously determining the kinetic energy and number of electrons that get-away from the top one to ten nm of the material being analyzed. Here, XPS measurements were measured for Ag_2O NPs to investigate the chemical states of Ag_2O. The XPS spectra of Ag3d, and O1s are presented in Fig. 3a. XPS was also used to resolve the chemical state of the doped Ag_2O NPs and their depth. Figure 3b presents the XPS spectra (spin-orbit doublet peaks) of the $Ag3d_{(5/2)}$ regions recorded with semiconductor doped materials. The binding energy of the $Ag3d_{(5/2)}$ peak at 368.3 eV denotes the presence of Ag_2O since their bindings energies are similar [64]. The O1s spectrum shows a main peak at 532.8 eV in Fig. 3c. The peak at 532.8 eV is assigned to lattice oxygen may be indicated to oxygen (ie, O_2^-) presence in the Ag_2O NPs [65]. XPS compositional analyses evidenced the existence of the two single-phase of Ag_2O

materials. Therefore, it is concluded that the thermo-chemically prepared Ag_2O have NPs phase contained silver oxide nanomaterials. Also, this conclusion is well-match with the XRD data perceptibly.

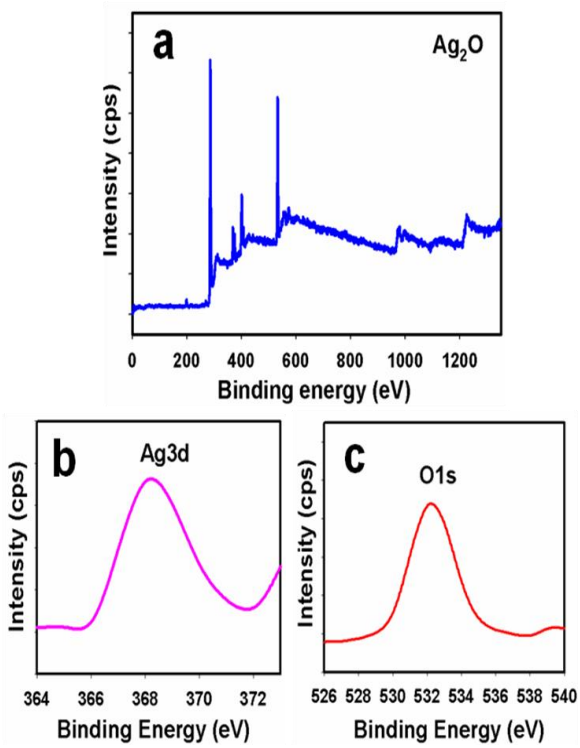

Figure 3. XPS of (a) Ag_2O NPs, (b) Ag3d level, and (c) O1s level acquired with MgKα radiation.

3.3. Detection of APPT antiemetic drug using Ag_2O/μ-Chips assembly

With high mechanical strength, good conductivity, large-surface area, and extremely miniaturized size of un-doped silver oxide nanoparticles have been widely employed in biomolecule detection. The as-grown nanoparticles were applied for the detection of Aprepitant in liquid phase system at room conditions. The potential application of Ag_2O NPs assembled onto μ-chip has been employed for measuring and quantifying APPT drug. Enhancement of undoped Ag_2O NPs on μ-chip as drug sensors is in the initial stage and no other reports are available. The NPs of Ag_2O fabricated electrodes have advantages such as stability in air, non-toxicity, chemical inertness, electro-chemical activity, simplicity to assemble or fabrication, and bio-safe characteristics. As in the case of APPT drug sensors, the phenomenon of reason is that the current response in electrochemical technique (I-V method) of Ag_2O NPs considerably changes, when buffered APPT is adsorbed. The Ag_2O NPs were applied for modification of drug sensor, where APPT was measured as target antiemetic drug analyte. The Ag_2O NPs are fabricated and employed for the detection of APPT drug in buffer phase. It is measured the I-V responses of Ag_2O NPs/μ-chips, which is presented in the **Scheme 1**. Platinum line (PtE) and gold-circle onto μ-chip are used as counter and working electrode (voltage sources on two electrode system) respectively, which is presented in the Scheme-1(a-c). The probable detection

mechanism of fabricated APPT drugs using I-V responses is presented in Scheme-1d. The experimental electrochemical (I-V) detection methods with NPs using conducting binder are presented in the Scheme-1e.

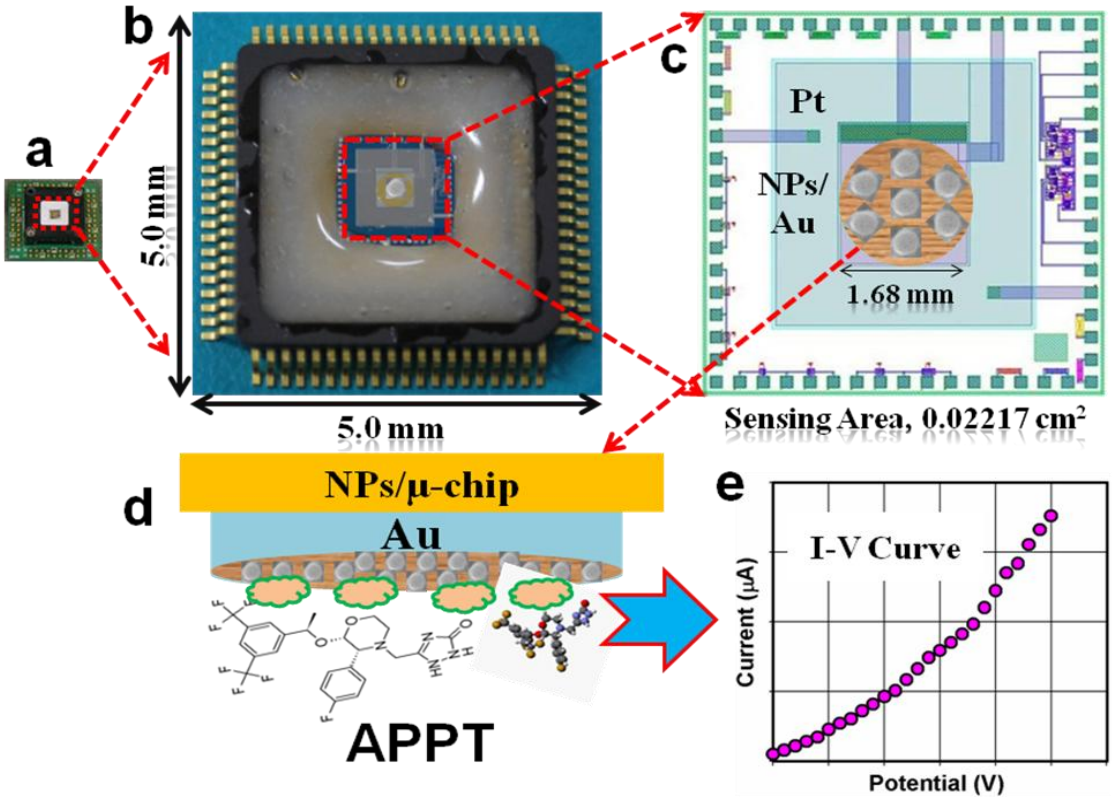

Scheme 1. Schematic diagram of (a) real camera-view from top of µ-chip, (b) magnified view of fabricated NPs/µ-chips, (c) magnified view of Ag_2O NPs/µ-chips with conducting binders (EC & BCA) onto sensing-area, (d) reaction mechanism of APPT drugs in presence of Ag_2O NPs, and (e) outcomes of I-V experimental results.

The fabricated-surface of Ag_2O NPs sensor was made with conducting binders (EC & BCA) on the µ-chip surface, which is already presented in the Scheme 1(a-d). The fabricated µ-chip electrode was placed into the oven at low temperature (65.0 ^oC) for 3 hours to make it stable and uniform the surface totally. I-V signals of APPT are anticipated having Ag_2O NPs on thin-film as a function of current versus potential for target drugs. The real electrical responses of target APPT are investigated by simple and reliable I-V method using Ag_2O NPs fabricated µ-chips, which is also presented in Scheme 1e. The holding time of electrometer was set for 1.0 sec. A significant amplification in the current response with applied potential is perceptibly confirmed. The simple and possible reaction mechanism is generalized in Scheme 1d in presence of APPT on Ag_2O NPs sensor surfaces by electrochemical approaches.

Figure 4a shows the current responses of without fabrication (gray-dotted) and with fabrication (dark-dotted) of µ-chips as working electrode surfaces with Ag_2O NPs. With NPs fabricated surface, the current signal is reduced compared to without fabricated µ-chip surface, which indicates the

modified surface is slightly inhibited with Ag_2O NPs. The current changes for the NPs modified film without (dark-dotted) and with (blue-dotted) injecting of 50.0 µL APPT (~0.123 µM) onto Ag_2O NPs modified µ-chips, which is showed in Figure 4b. This significant change of surface current is examined in every injection of the target APPT drug onto the Ag_2O NPs/µ-chips by electrometer. I-V responses with Ag_2O NPs modified µ-chip surface are investigated from the various concentrations (2.2 nM to 0.04 mM) of APPT, which is showed in Figure 4c. It shows the current changes of fabricated Ag_2O NPs/µ-chip films as a function of APPT concentration in room conditions. It was also found that at low-high concentration of target APPT, the current responses were increased slowly. The potential current changes at lower to higher potential range (potential, +0.01 V to +1.5 V) based on various APPT concentration are observed, which is clearly presented in Figure 4c. A large range of APPT concentration is executed with the probable analytical limit, which is calculated in 2.2 nM to 0.04 mM. The calibration curve was plotted from the variation of APPT concentrations, which is presented in the Figure 4d. The sensitivity is estimated from the calibration curve, which is close to ~2.732 $\mu Acm^{-2}\mu M^{-1}$. The linear dynamic range of this APPT drug sensor displays from 2.2 nM to 4.1 µM (linearity, R= 0.9852) and the detection limit was considered as 0.29 µM [3×noise (N)/slope(S)].

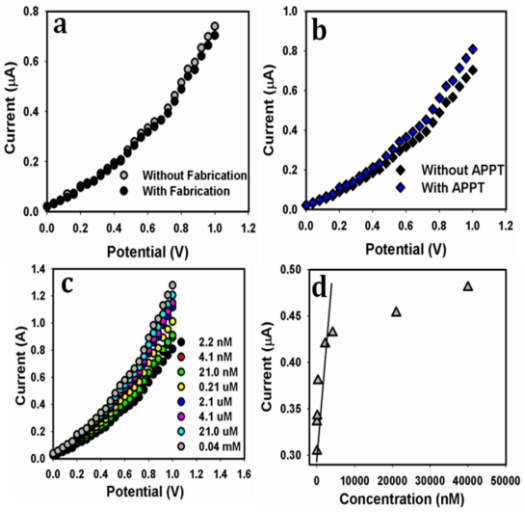

Figure 4. I-V responses of (a) without and with fabrication of µ-chip by Ag_2O NPs; (b) NPs/µ-chip (without APPT) and NPs/µ-chip (with APPT) (APPT solution dropped onto chip: ~2.2 nM); (c) concentration variations of APPT (2.2 nM to 0.04 mM) by NPs/µ-chip; (d) Calibration plot of Ag_2O NPs/µ-chip [current values are collected at +0.5V from Fig4(c)].

In buffer phase, the dependent on reactant constituents, mechanism of chemi-sorption, and further desorption of APPT analytes on the Ag_2O NPs/µ-chip surfaces were evaluated in details. The NPs/µ-chip is exhibited semiconductor behaviors, where the electrical resistance decreases under the presence of APPT reducing agent. The film resistance is decreased gradually (increasing the resultant current) upon increasing the APPT concentration in bulk phase. The analytical parameters of the NPs/µ-chip fabricated sensor are relatively better compared to previously reported APPT drugs, based on other nano-composite or nano-materials modified an electrode.

Table 1. Comparison of the analytical parameters of the proposed I-V method by Ag_2O NPs/μ-chip with earlier reported techniques for the detection of APPT

Materials	Methods	LDR	Sensitivity	LOD	r^2	Ref.
Pharmaceutical dosage	RP-HPLC method	0.99 to 101.5mM	79.976±0.12 uA uM^{-1}	0.130μg/ml	0.9997	[66]
Capsules Dosage	RP-HPLC	14-168 μg/ml	---	0.28 μg/ml	0.9999	[67]
Drug Substances	FTIR method	2-96 wt%	----	2.1 wt %	0.9719	[68]
Chemotherapy	Chromatog rhapy	up to 150 mg	0.80 mg/APT	1 mg/mL	---	[69]
Conventional therapy	midazolam probe	2-150mg//d	125/80-mg/d	125/80 mg	---	[70]
Pharmaceutical dosage	RP-HPLC	25-150 μg/ml	---	0.28μg/ml	0.9999	[71]
Iron oxide nanoparticles	I-V technique	2.2 nM to 4.0 μM	2.5316 uA $uM^{-1}cm^{-2}$	0.38 nM	0.9703	[72]
Ag_2O NPs/μ-chip	I-V method	2.2 nM to 4.1 μM	2.732 uA $uM^{-1}cm^{-2}$	0.29 nM	0.9852	Current work

The fabricated sensor response time was around ~10.0 sec for the Ag_2O NPs coated μ-chip sensor to achieve the saturated steady state current in I-V plots. The major sensitivity of Ag_2O NPs/μ-chip APPT sensor can be attributed to the good absorption (porous surfaces NPs fabricated with binders), adsorption ability, high-catalytic activity, and good bio-compatibility of the Ag_2O NPs/μ-chip. The expected sensitivity of the NPs fabricated APPT sensor is relatively better than previously reported drug sensors based on other composites or materials modified electrodes (Table 1). Due to large-surface area, here the undoped Ag_2O NPs proposed a beneficial nano-environment for the APPT drug detection (by adsorption) and recognition with excellent quantity. The prominent sensitivity of Ag_2O NPs/μ-chip affords high electron communication features which improved the direct electron communication between the active sites of Ag_2O NPs and μ-chips. The modified thin Ag_2O NPs/μ-chip sensor film had a better reliability as well as stability in ambient conditions. To check the reproducibly, response time, and storage stabilities, I-V response for Ag_2O NPs/μ-chip APPT sensor was examined (up to 2 weeks). After each experiment, the fabricated Ag_2O NPs/μ-chip substrate was washed thoroughly with the PBS buffer solution and observed that the current response was not significantly decreased. The response time is gradually increased with increasing the concentration of target analyte, which is less than 10.0 sec [73]. The sensitivity was retained almost same of initial sensitivity up to week (1^{st} to 3^{rd} week), after that the response of the fabricated micro-electrode gradually decreased. A series of six successive measurements of 2.2 nM APPT in 0.1 mM PBS yielded a good reproducible signal at Ag_2O NPs/μ-chip sensor with a relative standard deviation (RSD) of 3.8% (Figure not shown). The sensor-to-sensor and run-to-run repeatability for 2.2 nM APPT detection were found to be 1.8% using Ag_2O NPs/μ-chip. To investigate the long-term storage stabilities, the response for the NPs sensor was determined with the respect to the storing time. The long-term storing stability of the Ag_2O NPs/μ-chip drug sensor was investigated extensively. The sensitivity retained

93.0% of initial sensitivity for several days. The above results clearly suggested that the fabricated APPT sensor can be used for several weeks without any significant loss in sensitivity.

4. CONCLUSION

Finally, low-dimensional silver oxide nanoparticles are prepared by facile wet-chemical method with controlled morphology, which is exposed a constant morphological improvement in nanostructure materials and potential biomedical applications. Low-dimensional nanoparticles are allowed very sensitive transduction of the liquid/surface interactions for APPT detection at room conditions. This opportunity is to emergence a variety of structural morphologies proposed different approaches of modification of the drug biomolecules with silver oxide nanostructures. Here, nanoparticles are employed to fabricate a simple, efficient, and sensitive APPT detection consisting on fabricated microchip electrode surface. To best of our knowledge, this is the first report for detection of APPT antiemetic drug with silver oxide nanoparticles using simple and reliable I-V method in short response time. This approach has described for the detection of APPT with un-doped nanoparticles in various attractive and potential features.

ACKNOWLEDGEMENT
This paper was funded by King Abdulaziz University, under grant No. (T-001/431). The authors, therefore, acknowledge technical and financial support of KAU.

References

1. S. Namal, B.Z. Awen, B.R. Chandu, M. Khagg. *Recent Res. in Sci. Tech.* 3 (2011) 16.
2. L.A. Sorbera J. Castaner, M. Bayes, J. Silvestre. *Drug. Fut.* 27 (2002) 211.
3. K.C. Lasseter, J. Gambale, B. Jin, A. Bergman, M. Constanzer, J. Dru, T.H. Han, A. Majumdar, J.K. Evans, M.G. Murphy. *J. Clin. Pharmacol*. 47 (2007) 834.
4. K. Pendergrass, R. Hargreaves, K.J. Petty, A.D. Carides, J.K. Evans, K.J. Horgan. *Drug. Today*. 40 (2004) 853**.**
5. S. Poli-Bigelli, J. Rodrigues-Pereira, A.D. Carides. *Cancer*. 97 (2003) 3090.
6. R. de-Wit, P.J. Hesketh, D. Warr, *Am. J. Cancer*. 4 (2005) 35.
7. R. Helmy, G.X. Zhou, Y.W. Chen, L. Crocker, T. Wang, R.M. Wenslow, A. Vailaya. *Anal. Chem*. 75 (2003) 605.
8. A.M. Griffin, P.N. Butow, A.S. Coates. *Ann. Oncol.* 7 (1996) 189.
9. J.J. Hale, G.M. Sander, M. MacCoss, P.E. Finke, P.J. Hesketh, M.A. Cascieri, S. Sadowski, E. Ber, G.G. Chicchi, M. Kurtz, J. Metzger, G. Eiermann, N.N. Tsou, F.D. Tattersall, N.M.J. Rupnaik, A.R. Williams, W. Rycroft, R. Hargreaves, D.E. MacIntyre. *J. Med. Chem*. 41 (1998) 4607.
10. R.M. Navari, R.R. Reinhardt, R.J. Gralla, M.G. Kris, P.J. Hesketh, A. Khojasteh, H. Kindler, T.H. Grote, K. Pendergrass, S.M. Grunberg, A.D. Carides, B. Gertz. *J. New Eng. J. Med.* 340 (1999) 190.
11. H.A. Lieberman, L; Lachman, J.B. Schwartz, *Pharmaceutical Dosage Forms: Tablets,* 2nd ed.; Marcel Dekker: New York, 1990; 1-3.
12. J.S. Peter, A. Ahmed, W. Yan. *J. Pharm. Biomed. Anal*. 41 (2006) 883.
13. D. Wu, J.P. Dustin, Z. Xianguo, D. Steven, S.B. Jeffrey. *J. Pharm. Biomed. Anal*. 49 (2009) 739.

14. H. Roy, X. George, W. Yadan, C. Louis, W. Tao, M. Robert, V. Anant. *Anal. Chem*. 75 (2003) 605.
15. L. Dupuis, L. Karen, W. Lingertat E.W. Scott. *Sup. Car. Can.* 17 (2009) 701.
16. V.K. Kumar, N.A. Raju, S.H. Begum, J.V.L.N.S. Rao. *Res. J. Pharm. Tech*. 2 (2009) 412.
17. K.K. Caswell, C.M. Bender and C.J. Murphy, *Nano Lett.,* 3 (2003) 667-669.
18. D. Adukondalu, P. S. Malathy, J.V. Rao and Y.M. Rao., *IJPBS*, 1(2011)474-478.
19. M.M. Rahman. *Current Proteom.*, 9(2012)272-279.
20. A. Graff, D. Wagner, H. Ditlbacher and U. Kreibig, *Eur. Phys. J., D at. Mol. Opt. Phys*., 34 (2005) 263-269.
21. M.M. Rahman, A. Umar and K. Sawada. *Sens. Actuator: B Chem*., 137 (2009) 327-333.
22. M.M. Rahman, A. Jamal, S.B. Khan, M. Faisal and A.M. Asiri. *Chem. Engineer. J.*, 192 (2012) 122-128.
23. D. Srinivasulu, B.S.Sastry, G. Omprakash., *Int. J. Chem. Res*., 1(2012)18-20.
24. M.M. Rahman. *J. Biomed. Nanotech*., 7 (2011) 351-357.
25. M.M. Rahman. *Intern. J. Biolog. Med. Res*., 1 (2010) 9-14.
26. F. Faridbod, M.R. Ganjali, E. Nasli-Esfahani, B. Larijani, S. Riahi and P. Norouzi., *Int. J. Electrochem. Sci*., 5 (2010) 880 – 894.
27. N.A. Al-Arfaj, E.A. Al-Abdulkareem and F.A. Aly., *Anal. Sci.* 25(2009)401-406.
28. S. Balendhran, S. Walia, M. Alsaif, E.P. Nguyen, J.Z. Ou, S. Zhuiykov, S. Sriram, M. Bhaskaran and K. Kalantar-zadeh., *ACS Nano*, 7(2013)9753–9760.
29. S. Liu, J. Yue and A. Gedanken, *Adv. Mater*., 13 (2001) 656-658**.**
30. S.R. Lee, M.M. Rahman, M. Ishida and K. Sawada. *Biosens. Bioelectron*., 24 (2009) 1877-1882.
31. A. Dıaz-Parralejo, R. Caruso, A.L. Ortiz and F. Guiberteau. *Thin Sol. Film*, 458 (2004) 92–97.
32. S.R. Lee, M.M. Rahman, M. Ishida and K. Sawada. *Trends in Anal. Chem.,* 28 (2009) 196-203.
33. G.A.E. Mostafa and A. Al-Majed., *J. Pharmaceut. Biomed. Anal.,* 48(2008)57–61.
34. M. Wang, I.R. Miksa, *J. Chromatogr. B,* 856 (2007) 318.
35. L. Zhang, Y. Tian, Z. Zhang and Y. Chen, *J. Chromatogr. B*, 854 (2007) 91.
36. W. Zeng, D. Musson1, A.L. Fisher, L. Chen, M.S. Schwartz, E.J. Woolf, A.Q. Wang, *J. Pharm. Biomed. Anal*., 46 (2008) 534.
37. P. Sripalakit, P. Neamhom and A. Saraphanchotiwitthaya, *J. Chromatogr. B,* 843(2006) 164.
38. M.M. Rahman, A. Jamal, S.B. Khan and M. Faisal. *Biosens. Bioelectron*., 18 (2014) 127-134.
39. G.A.E. Mostafa and A. Al-Majed, *J. Pharm. Biomed. Anal.,* 48 (2008) 57.
40. R.I. El-Bagary, E.F. Elkady and B.M. Ayoub, *Int. J. Biomed. Sci.,* 7 (2011) 201.
41. S. AbuRuz, J. Millership and J. McElnay, *J. Chromatogr. B,* 817 (2005) 277.
42. J. Keal and A. Somogyi, *J. Chromatogr*., 378 (1986) 503.
43. A. Liu and S.P. Coleman, *J. Chromatogr. B,* 877 (2009) 3695.
44. N. Koseki, H. Kawashita, M. Niina, Y. Nagae and N. Masuda, *J. Pharm. Biomed. Anal.,* 36 (2005) 1063.
45. H.M. Asif, T.R. Rao and M. Anjum. *Inter. J. Pharm. Pharmac. Sci.,* 6(2014)91-96.
46. P. Deepak, J. Abhishek, J. Rakesh K. and S. Hariharanand. *Inter. J. Drug Discovery Herbal Res*., 1 (2011) 157-163.
47. O. Wilson, G.J. Wilson and P. Mulvaney, *Adv. Mater.,* 14 (2002) 1000-1004.
48. M.M. Rahman *Plos One*, 9 (2014) e100327.
49. Z.H. Cai and C.R. Martin, *J. Am. Chem. Soc*., 111 (1989) 4138-4139.
50. A. Tao, F. Kim, C. Hess, J. Goldberger, R. He, Y. Sun, Y. Xia and P. Yang, *Nano Lett.,* 3 (2003) 1229-1231.
51. Z. Zhang, D. Gekhtman, M.S. Dresselhaus and J.Y. Ying. *Chem. Mater.,* 11 (1999) 1659-1662.
52. A. Kipke and H. Hofmeister. Mater. Chem. Phys., 111 (2008) 254-259.
53. A.P. Karpinski, S.J. Russell, J.R. Serenyi, J.P. Murphy. *J. Pow. Source* 91 (2000) 77-82.
54. D.F. Smith and J.A. Gucinski, *J. Pow. Sour.,* 80 (1999) 66-71.

55. M.S. Antelman, *US Patent* (1993) 5.211.855.
56. F. Di-Fonzo, M.P. Bogana, D. Dellasega, A. Facibeni and C.E. Bottani, *Italian Patent* (2007) MI2007A000683.
57. J. Pan, Y. Sun, Z. Wang, P. Wan, X. Liu and M. Fan, *J. Mater. Chem*., 17 (2007) 4815-4820.
58. J.J. Zhu, S.W. Liu, O. Palchik, Y. Koltypin and A. Gedanken, *Langmuir* 16 (2000) 6396-6399.
59. F. Xu, Y. Zhang, Y. Sun, Y. Shi, Z. Wen and Z. Li. *J. Phys. Chem. C*, 2011 (115) 9977–9983.
60. G. Shen and D. Chen, *J. Phys. Chem. C*, 2010 (114) 21088–21093.
61. Y. Pan, J. Gao, B. Zhang, X. Zhang and B. Xu, *Langmuir*, 2010 (26) 4184–4187.
62. R. Brenier, *J. Phys. Chem. C*, 2009 (113) 1758–1763.
63. B.J. Privett, S.M. Deupree, C.J. Backlund, K.S. Rao, C.B. Johnson, P.N. Coneski and M.H. Schoenfisch, *Mol. Pharmaceutics*, 2010 (7) 2289–2296.
64. S. Bhattacharyya and A. Gedanken, *J. Phys. Chem. C*, 2008 (112) 659–665.
65. B.H. Hong, S.C. Bae, C.W. Lee, S. Jeong and K.S. Kim, *Science*, 294 (2001) 348-351.
66. S. Nama, B.Z. Awen, B.R. Chandu, M. Khagga. *Recent Res. Sci. Tech*. 3 (2011) 16-24.
67. V.K. Kumar, N.A. Raju, S. Begum, J.V.L.N.S. Rao, T. Satyanarayana. *Res. J. Pharm. Tech.*
68. 2(2009) 412-414.
69. R. Helmy, G.X. Zhou, Y.W. Chen, L. Crocker, T. Wang, R.M. Wenslow, A. Vailaya.
70. *Anal. Chem*. 75 (2003) 605-611.
71. K.C. Lasseter, J.G. Pharm, B. Jin, A. Bergman, M. Constanzer, J. Dru, T.H. Han, A. Mujumdar,
72. J.K. Evans, M.G. Murphy. *J. Clinical Pharm*. 47 (2007) 834-840.
73. Majumdar. *Clinic. Pharm. Therap*. 74(2003)150-156.
74. K.K. Chaitaniya, D.G. Sankar, D.S. Israel, C.N. Kumar. *Der Pharm Chemica* 5(2013)39-46.
75. M.M. Rahman, S.B. Khan, M. Faisal. A.M. Asiri and M. A. Tariq. *Electrochim. Acta*, 75 (2012) 164–170.
76. Z.H. Dhoondia and H. Chakraborty. *Nanomater. Nanotechnol*., 2 (2012) 15.